TREE JOINTS: BIOMIMETIC INSIGHTS FOR AEROSPACE COMPOSITE JOINTS

L.A. Burns*
PhD Candidate, RMIT University
Supervisors: *Dr S. Feih (RMIT University), Prof. A. Mouritz (RMIT University), Mr D. Pook (Boeing Research and Technology Australia)*

Keywords: *Biomimetic, Biomimicry, Tree, Composite, Joints*

Abstract

The purpose of this study is to improve the mechanical properties of aerospace composite joints by biomimicry of evolutionarily optimized tree joints. The study involved an experimental investigation with the aim of gaining insights into the structure and mechanical properties of tree joints. Carbon epoxy biomimetic prototypes were tested and compared to conventionally designed aerospace composite joint design.

The bending strength and failure modes of branch-trunk joints from the species Pinus radiata *were investigated. Despite the intrinsic brittleness of the constituents of the wood composite, tree joints achieve an elastic-plastic stress response with high toughness. Under gravity direction bending the tree joints fractured along a cone-shaped surface. Scanning Electron Microscopy (SEM) and Micro CT revealed that the micro-structure at the joint is adapted to achieve high toughness through a sophisticated 3D fiber placement and significant fiber bridging and fiber pullout. CT showed qualitatively that the wood density varies across the joint, with the highest fiber volume fraction in the areas of maximum stress.*

Conventional and biomimetic T-joints with 25% of the stiffener plies embedded into the skin were fabricated and tested under tensile, bending and compression loading. The biomimetic T-joint showed a 27% improvement in average bending load and no change in strength under tensile and compressive loading.

1 Introduction

1.1 Aircraft Composite Joints

Joints and interfaces are one of the key aspects of aircraft design and production. An aircraft is assembled using many thousands of joints, which are often the weakest link within the structure. Strength, stiffness, toughness and design life are some of the most important mechanical properties of aerospace joints [1].

Designers of modern composite airframes have realised the advantage of orthotropic composites, which can be tailored to align the strong longitudinal fibers with the primary load direction, resulting in significant weight savings in parts such as aircraft skins. Paradoxically, designers have persisted in joining composite parts using traditional methods originally developed for isotropic metallic structures. Composite parts are frequently joined using bolts and rivets. The main disadvantage of this approach is that it destroys the load bearing fibers and does not distribute the load uniformly, resulting in high local stresses in areas already weakened from severed fibers [2].

Composite joints designed without fasteners, using either adhesives or co-curing of components, also present challenges. The main problem is developing a safe design that can resist through-thickness stresses while avoiding rapid, brittle and catastrophic failure of the joint when it exceeds the design load. The fear of rapid brittle failure or ‘unzipping’ of bonded joints results in conservative designs, negating the weight-saving potential of composites.

Failure to develop optimised aircraft composite joints generates a weight penalty due to the need for reinforcing plies and fasteners. This reduces the efficiency of the design, thus

increasing the environmental, manufacturing and operating costs of the aircraft.

1.2 Background to Biomimetics

'Biomimetics' is the science of imitating nature. An aerospace related example is the aerodynamic improvement gained from the 'shark skin effect.' Shark skin has grooved scales directed almost parallel to the body axis of the shark, with the corrugations affecting the viscous boundary layer of water. An A-340 was fitted with a similar ribbed structure, reducing aircraft drag by 8% [3].

1.3 Designing from Trees and Wood

Trees and wood were selected for investigation because of the following similarities in structure to aerospace composite materials;

- Trees have non-articulated joints that undergo a combination of static and dynamic loading as a result of self-weight, snow and wind.
- Wood is a highly orthotropic composite comprised of cellulose fibers in a hemi-cellulose/lignin polymer matrix.
- The double cell wall can be modelled as a 7 ply balanced laminate.
- Wood cells (grains) are laid down in a complex 3D lay-up that is nevertheless consistent with the principles of aerospace composite manufacturing.

The main determinant of wood mechanical properties is the angle of the helically wound cellulose micro-fibrils in the (main) S2 cell wall as shown in Figure 1. Lower angles (in relation to the longitudinal cell axis) signify better tensile strength and stiffness, while higher angles signify better fracture toughness and resistance to buckling [4].

Jeronimidis [5] found that the fracture energy of wood in the transverse (radial and tangential) direction is many orders of magnitude higher than its free surface energy. The high work of fracture of wood is due to the arrangement of the cellulose microfibrils in the S2 wood cell wall. The helically wound pattern of these fibrillae induce a novel form of buckling failure in tension, which produces an elastic behaviour analogous to the yield point of ductile metals.

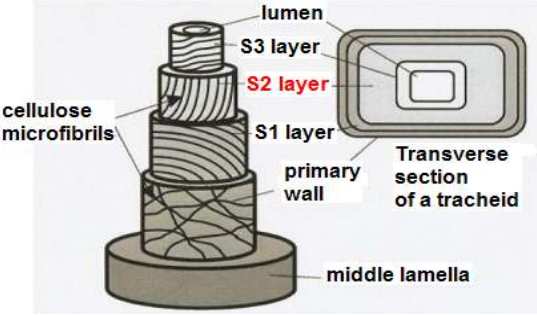

Figure 1 Structure of the wood cell wall [4]

Shigo [6] examined the structure of the branch-trunk joint and determined that branch wood grows directly into the trunk on the underside of the branch only. Branch tissues develop first, early in the growing season. Later the trunk tissues form a collar about the branch, resulting in a 'ball and socket' union. Mueller et al. [7] measured branch joint strains directly using 3D electronic speckle pattern interferometry (ESPI). It was found that the tree joint had a small and almost homogeneous strain field. This suggests the tree joint has evolved to the axiom of uniform strain, which is advantageous because no particular location is prone to crack nucleation. It was proposed that uniform strain is achieved through; i) Fiber placement; ii) Variation in material properties across the joint; iii) Optimized notch shape. Further investigation by Jungnikl et al. [8] confirmed that the mechanical properties of wood vary across the joint, depending on the loading conditions. Variations in stiffness, strength and fracture toughness are primarily achieved through a change in the micro-fibril angle of the S2 layer of the cell wall. The effects of the micro and macro-level tree joint structure on the fracture mechanics of the tree joint under its intended loading direction have not been studied in detail.

The homogeneous strain response, ductility and toughness of tree joints are important properties that are currently not replicated in conventional aerospace T-joints fabricated using carbon fiber-epoxy composites. This paper aims to study the mechanical properties, failure modes and toughening

mechanisms of tree joints at the micro-structural and macro-levels in order to obtain information that can be adapted back into the design of aerospace composite joints. It is hypothesized that mimicking these concepts will result in improved structural performance of carbon epoxy T-joints.

2 Experimental Method

2.1 Branch-Trunk Joint Bending Testing

24 branch-trunk joints from the species *Pinus Radiata* were obtained from Hancock Victorian Plantations in Gippsland, Victoria (Location: 146.217˚ E, 38.217˚ S). The specimens were from three different trees, which were all planted in 1994. *Pinus Radiata* was chosen as a softwood representative of many other softwood species and these particular specimens had a common age and growth history.

The morphology of the specimens was characterized, including the branch angle to the trunk (from vertical): (Range: 46 – 88˚. Av: 72˚), branch diameter: (Range: 17 – 45 mm. Av: 30 mm) and trunk diameter: (Range: 22 – 159 mm. Av: 93 mm). The tree joint samples all had a moisture content of about 30%, consistent with green or freshly cut wood.

A test rig was developed as shown in Figure 2. The distance from the centre of the loading strap to the base of the branch (moment arm) was measured. The strap was connected to an Instron 50 kN machine, which applied a bending load to the branch via the strap.

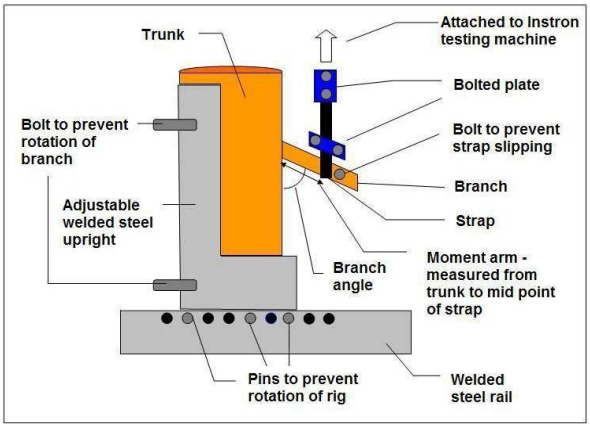

Figure 2 Schematic of branch bending test rig

Branches were tested under 'natural' loading in the gravity load direction. Branches were tested as intact or bisected samples. The bending stress at the joint was calculated according to the engineering flexure formula:

$$\sigma_{\max} = \frac{My_{\max}}{I_{xx}} \quad (1)$$

$\sigma_{\max}$ = max bending stress at branch junction (MPa)
M = bending moment at branch junction (N.mm)
$y_{\max}$ = max vertical distance from neutral axis of branch at junction (mm)
I_{xx} = Moment of inertia at the branch junction (mm^4)

It was assumed that the cross-sectional areas of the bend branch remained plane. Although the requirement for a homogenous material is not fulfilled in the tree joint (as shown by Jungnikl et al. [8]) it can be used as a good approximation for a comparison.

2.2 Tensile, Bending and Compression Testing of Carbon Epoxy T-Joints

Conventional and biomimetic T-joints were fabricated from carbon epoxy satin weave fabric pre-preg (Hexcel AGP370-5H/3501-6) and cured in the autoclave at 180ºC for 2 hours at 100 psi. For both designs the skin lay-up was 8 ply quasi isotropic [+/-45, 0/90, +/-45, 0/90] and the stiffener lay-up was 8 ply [+/-45, 0/90, 0/90, +/-45]. The void under the stiffener radius bend was filled with a plug consisting of 4 layers of 10 mm width fabric pre-preg. The biomimetic prototype had 25% of the stiffener plies embedded into the skin as shown in Figure 3B. This design was based on the observed structure of the tree joint shown in Figure 3C**.** It was hypothesized that embedding part of the stiffener into the skin would benefit the transfer of shear stresses from the stiffener into the skin and may also disperse crack growth and increase toughness. However the reduction in continuous fibers may correspondingly weaken the strength of the skin. The T-joints were tested under tension, bending and compression loading configurations as shown in Figure 5.

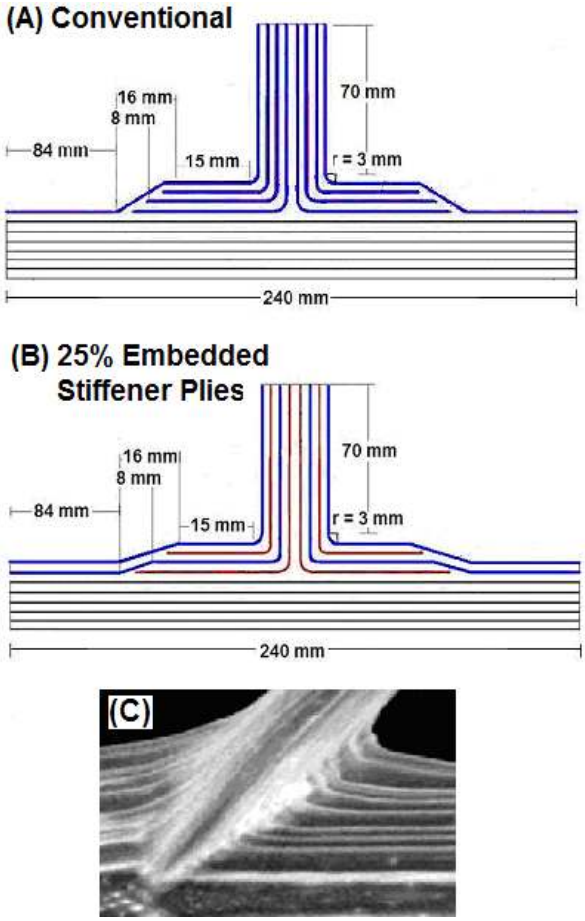

Figure 3 (A) Conventional T-joint design; (B) Biomimetic design: 25% of stiffener plies embedded into the skin; (C) Biomimetic inspiration from branch integration into tree trunk. Note: Density of branch varies from highest (brightest) at the outer diameter to lowest at the heart of branch, indicating a variation in fiber volume fraction

The difference in lay-up between the conventional and 25% embedded prototype resulted in different geometric properties, which are summarised in Table 1. In both designs the vertical stiffener had the same number of plies (8). However there was a difference in thickness, suggesting the biomimetic prototype had a lower fibre volume fraction in the stiffener. The stiffener flange/skin interface consisted of 12 plies in the conventional design, but only 10 plies in the 25% embedded stiffener design. To account for this difference the loading results were normalised with respect to the area of the flange/skin interface, which was calculated as $(t_1 + t_2)/2 \times w$.

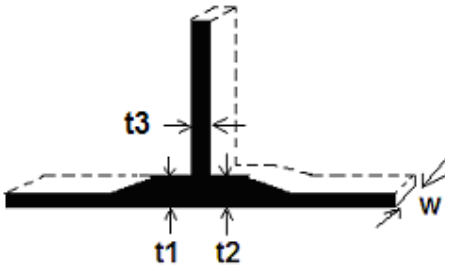

Figure 4 T-joint dimensions

	t_1 (mm)	t_2 (mm)	t_3 (mm)	w (mm)
Conv.	3.94	3.98	2.82	21.2
25%	3.69	3.72	3.03	20.8

Table 1 Comparison of T-joint dimensions

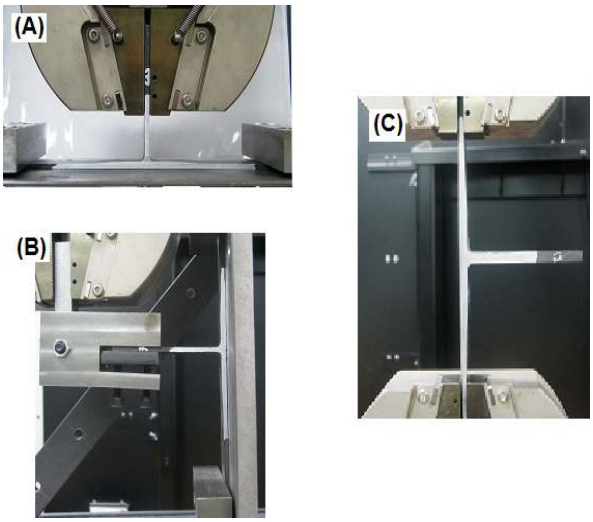

Figure 5 Loading configurations on 50 kN Instron testing machine; (A) Tension load on stiffener; (B) Bending load on stiffener); (C) Compression load on skin

3 Results and Discussion

To understand and evaluate the mechanics of the branch fracture it was first necessary to understand the structure. The tree joint could then be compared and contrasted to the structure and mechanical performance of the aerospace T-joint designs. The internal structure of two branch joints (one intact and one broken under gravity direction bending) were analysed by Computer Tomography (CT), performed using a Siemens Somatom Sensation 64 at Central Melbourne Medical Imaging. The specimens were scanned in a number of orientations with a

slice width of 0.5 mm, producing about 100 images for each through-thickness scan.

The CT scans and tree joint bending tests confirmed the description that branch wood for *Pinus radiata* grows directly into the trunk on the underside of the branch only [6]. This contrasts with conventional aerospace T-joints, which are designed to have continuous fibers running in both directions from the stiffener into the skin (Figure 3A).

The branch tissue of the tree joint is embedded to the centre of the trunk (Figure 6), contrasting with the conventional T-joint where the adherends remain separate. Figure 6 also illustrates the three-dimensional cone shape of the internal branch wood embedded in the trunk. This cone structure means there is no un-reinforced void at the interface of the tree branch-trunk joint. This contrasts with the conventional aerospace design, where the radius bend creates a significant region devoid of fibers that is resin rich and normally filled with a pre-preg plug or adhesive. This is often the weakest point within the aircraft joint and the location of failure initiation.

Figure **7 s**hows a front and side CT view of the tree joint. The trunk tissues extend forward and sideways to encase the branch, resulting in a 'ball and socket' union, shown schematically in Figure 8. A consequence of the ball and socket arrangement is a feature designated the 'joint seam', also illustrated in Figure 8. The joint seam is the interface of the branch and trunk wood. It is actually a grain stagnation point where, instead of intersecting, branch and trunk fibers turn 90˚ to one another. When viewed in cross section, the joint seam appears as a diagonal line running along the internal structure of the branch to the center of the trunk, reflecting the growth history of the branch. The joint seam is significant because it shows that tree joints have evolved *without continuous fibers* at the critical location of maximum tensile stress between the branch and the trunk. Trees have evolved to rely only on the transverse strength between fibers within the joint. Some branches are very large and heavy, yet they manage to sustain their self-weight and resist high wind loads in this configuration.

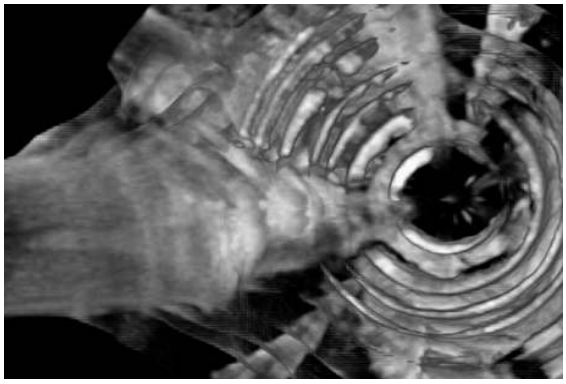

Figure 6 Plan view of tree joint showing cone-shaped ('V notch') branch wood extending to centre of trunk

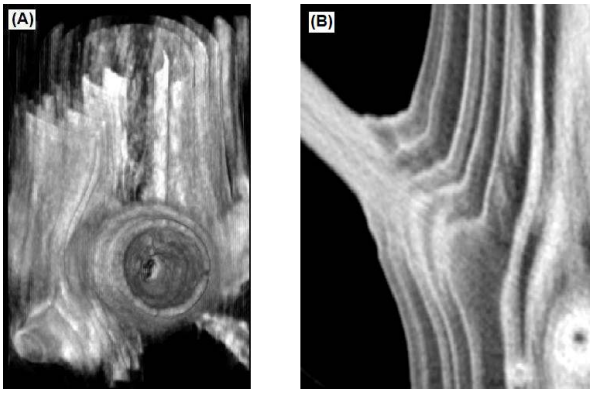

Figure 7 CT scan showing internal 3D fiber lay up of tree joint. (A) Front view: Trunk fibers extend laterally around the branch; (B) Trunk fibers extend forwards around the branch; Internal branch wood interfaces with trunk wood rings that flow forward and sideways to encase the branch in a collar or 'ball and socket' joint

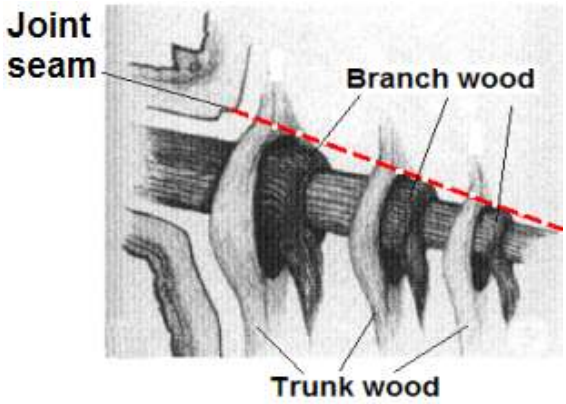

Figure 8 Schematic illustration of 3D 'ball and socket' arrangement of trunk wood encasing branch wood. The joint seam is shown as a dashed line following the interface of the branch and trunk wood in the internal branch structure [6]

Figure 3C shows high-density areas corresponding to bright spots in the areas of highest bending stress at the outer perimeters of the branch. This can be interpreted as a variation in the fiber volume fraction (V_f) across the joint, which is not currently a feature of aerospace composite joint design.

Representative bending results of the intact tree joint specimens under natural (gravity direction) loading are shown in Figure 9. Features include

- Initial linear region with similar stiffness
- Work hardening after linear region
- Ductile failure with significant residual strength after exceeding maximum stress
- High toughness
- Large variation in strength

This graph shape is more representative of an elastic-plastic material, such as a ductile metal. A major finding of the testing is despite the brittleness of the fiber constituent (cellulose) of the wood composite, the tree joint achieved a ductile failure. The arrangement of the wood fibers enabled the joint to overcome the brittleness inherent in most fiber polymer composites. Understanding the mechanism by which this occurred is a key issue in the biomimetic design of aerospace joints.

The composite T-joints failed in bending in one of two failure types. In Type 1 failure (Figure 10) the joint sustained no damage up to a high displacement and load and then experienced an entirely brittle failure whereby simultaneously each ply in the radius bend of the tension side of the joint delaminated and a crack propagated across the plug, resulting in a large load drop. In Type 2 failure (Figure 11) the joint sustained more gradual damage that occurred at a lower displacement and load. First damage was a delamination between ply 4 and the plug, followed by further delaminations and final failure when the crack propagated across the plug. The sensitivity of the joint between these two failure types resulted in a high standard deviation for the bending peak load.

Final failure illustrating the radius bend delaminations and the main crack across the plug is shown in Figure 12. There was a difference noted between the two joint designs in their tendency towards each failure mode.

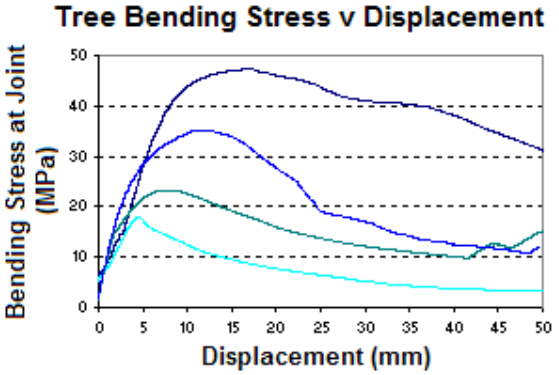

Figure 9 Stress response of intact tree branch-trunk joints under natural (gravity direction) bending

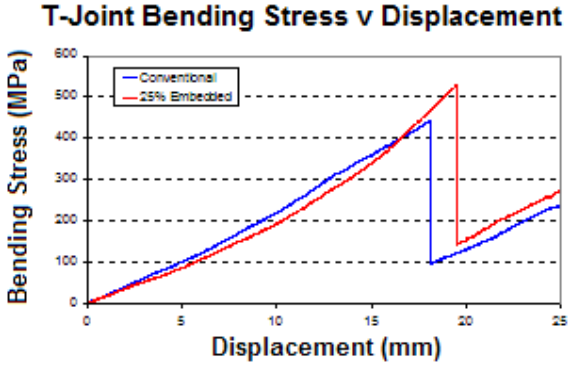

Figure 10 T-joint Type 1 bending failure

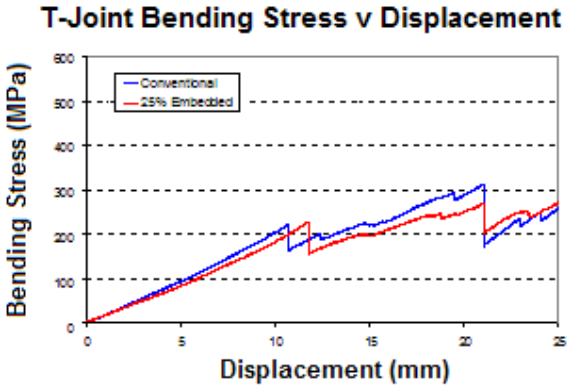

Figure 11 T-joint Type 2 bending failure

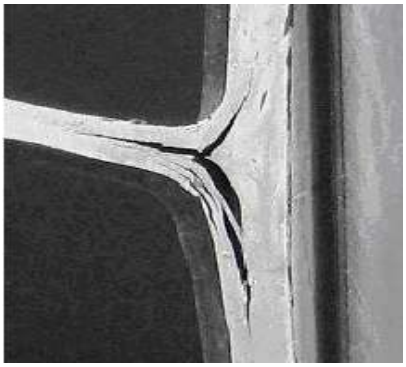

Figure 12 Failure of carbon epoxy T-joint under bending

In the conventional design 2/8 (25%) of samples experienced Type 1 failure, compared to the biomimetic design, where 6/9 (67%) of samples experienced Type 1 failure. As a result, the biomimetic design showed an average 27% increase in bending peak load compared to the conventional design. The improvement in bending strength may be due to changes in the peak stresses in the crucial radius bend/plug zone. This could be confirmed by examining the strain map of this area through direct strain measurement techniques, such as electronic speckle pattern interferometry (ESPI).

In the other load cases of tension and compression there was no significant difference between the failure modes and performance of the two T-joint designs (Figure 13).

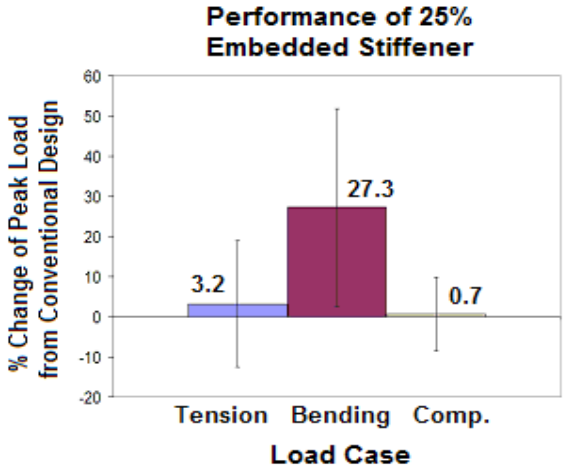

Figure 13 Comparison of static strength of biomimetic prototype with 25% embedded plies to conventional design. Error bars represent +/- 1 standard deviation of peak load as a percentage of average peak load for 25% embedded stiffener design

Load Case	T-joint design	Av. Peak Load (N)	Standard Deviation (N)	Load/ flange area (N/mm2)
Tension	Conventional	1186	178	14.30
	Biomimetic	1132	179	14.8
Bending	Conventional	91.3	25.3	1.09
	Biomimetic	106	26.1	1.40
Comp.	Conventional	5021	115	59.9
	Biomimetic	4636	426	60.3

Table 2 Average peak load, standard deviation and peak load/flange area for each load case and composite T-joint design

The failure mode of tree branches undergoing gravity direction bending was consistent with the structural features illustrated by the CT scans. Initial damage occurred on the tensile (top) side of the branch joint with a crack forming and propagating in a two-dimensional path around the branch circumference (Figure 14). This corresponded to the work hardening area of the stress curve.

As loading continued, the crack began to also propagate along the internal branch joint seam (Figure 15), corresponding to the ductile failure zone of the stress curve. There are no continuous fibers across the joint seam, making it is the path of least resistance for the crack to follow. This joint seam (Figure 16) was not always located in the geometric centre of the branch, indicating the flexible response of tree branches in adapting to unique loading conditions. During testing, specimens with the joint seam aligned with the vertical load direction exhibited the highest bending strength.

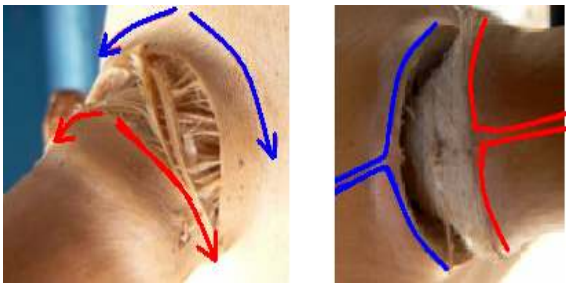

Figure 14 Left: Initial failure mode under gravity bending showing crack propagating around branch circumference; Right: Illustration of 'joint seam' at branch-trunk joint. Red lines = branch wood approaching trunk and turning 90˚; Blue lines = trunk wood approaching branch and turning 90˚

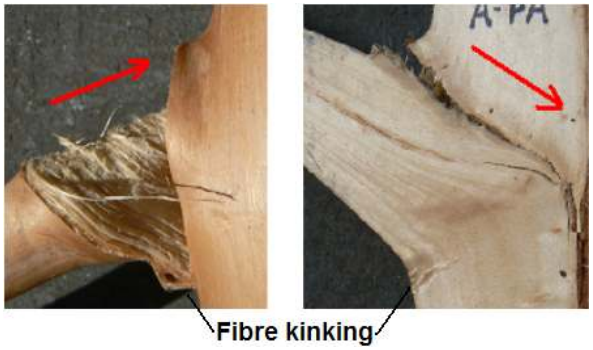

Figure 15 Arrows indicate direction of crack propagation along joint seam. Fiber kinking on the lower (compression) side of the joint is indicated

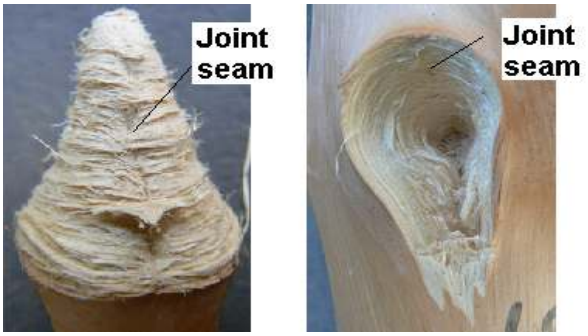

Figure 16 Tree joint fracture surfaces under gravity direction bending. The joint seam on both the branch and trunk is indicated

The three-dimensional cone-shaped (or V notch) branch fracture surface is one of the keys to understanding the toughness and ductility of the tree joint. The fracture occurs over the whole area of the cone, thus diffusing the load over a larger area and lowering the stress on the joint. The lack of continuous fibers across the cone-shaped joint seam also act as a strategic point of weakness, transferring the tensile stresses experienced under bending into a shear stress by deflecting the crack on about a 45˚ angle. This is advantageous because King et al. showed that saturated (freshly cut) *Pinus radiata* wood has 2 – 11 times higher fracture toughness in Mode II (shear) crack propagation compared to Mode I (opening) [9].

The fracture surface contained loose fibers (Figure 18) with a rough texture and was also corrugated, which increased the length of the crack path and created a mechanical interlocking mechanism that opposed the sliding and pullout of the branch fracture surface. Complete failure occurred when the branch cone pulled out completely, only remaining attached via the continuous fibers on the lower (compression) side of the branch. The compression side also exhibited fiber kinking after the crack on the tension side was established (Figure 15).

The intact and the bisected tree joint specimens both exhibited the same failure mode and similar strength, but the intact specimens had significantly better toughness, manifested in higher residual strength after maximum stress was exceeded (Figure 17). It is hypothesized that this is because the act of bisecting the joint interferes with the 'ball and socket' arrangement described by Shigo [6], and also destroys the integrity of the cone shaped fracture surface formed by the joint seam.

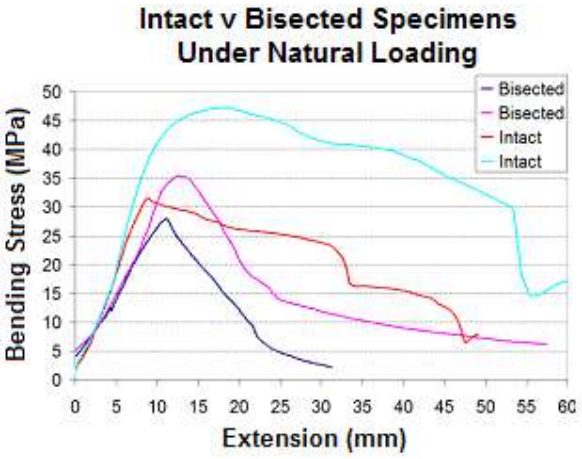

Figure 17 Performance of intact v bisected tree joints under bending

In contrast, under bending load the composite T-joints failed in the tensile radius bend of the stiffener and the resin rich plug (Figure 20). Despite the improvement in load carrying capacity the 25% embedded T-joint did not mimic the toughness and damage tolerance of the tree joint. This was due to the brittleness of the resin-rich plug zone. Controlling crack growth through this area is key to increasing the toughness of the joint. This may be achieved by altering the stiffener to mimic the V-shaped notch observed in the internal structures of the tree branch-trunk joint.

Scanning Electron Microscopy (SEM) of the tree joint bending fracture surface revealed heavy fiber bridging as a result of fiber pullout (Figure 18). Fiber pullout is a damage mechanism that absorbs a large amount of energy. Micro CT images of the tree branch-trunk joint (Figure 19) showed significant fiber bridging along the crack path. These fibers carry some of the load, thereby reducing the stress at the crack tip and increasing the toughness of the joint [10]. In contrast the aerospace composite joints tended to split without fiber bridging due to the pre-preg lay-up, concentrating the load at the crack tip, which resulted in unstable crack growth and brittle failure [10].

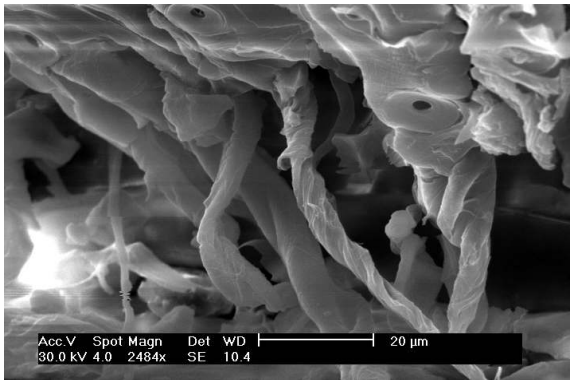

Figure 18 SEM of branch bending fracture surface showing fiber pullout and fiber bridging

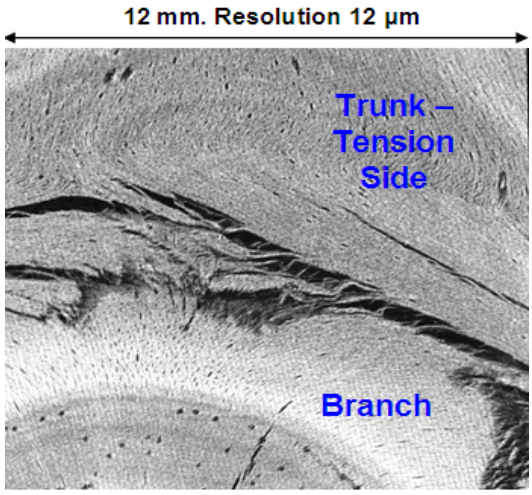

Figure 19 Micro-CT of front view of branch bending fracture surface showing fiber bridging.

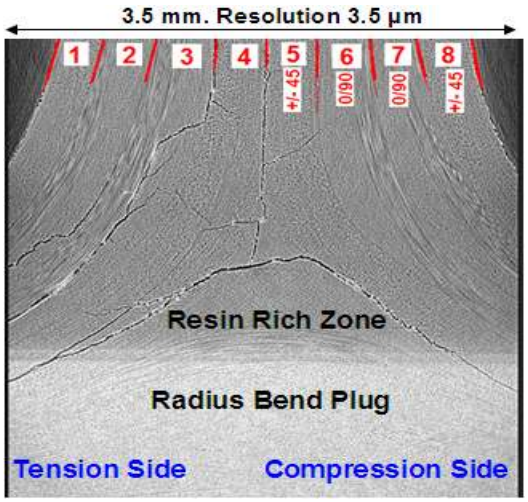

Figure 20 Micro-CT of front view of 25% embedded carbon epoxy T-joint bending fracture surface showing failure at resin-rich zone and inter and intra-laminar cracking on tensile side

4 Concluding Remarks

Computer Tomography (CT) scans demonstrated that the tree joint is more highly integrated than the conventional aerospace carbon-epoxy T-joint. In response, conventional and biomimetic prototypes (with 25% of the stiffener plies embedded into the skin) were fabricated and tested under tensile, bending and compressive loading. The biomimetic prototype showed an average 27% improvement in bending peak load in comparison to the conventional design, with no significant change in tensile and compressive loading strength.

Bending tests on the tree joints revealed the stress response is similar to an elastic-plastic material. There is an initial linear elastic region followed by work hardening and ductile failure. Tree joints are tough despite the fiber constituent (cellulose) being intrinsically brittle. In comparison, both the conventional and biomimetic carbon epoxy T-joints failed in bending in a brittle manner across the resin-rich plug. However the biomimetic T-joints more commonly failed at a higher load and displacement compared to the conventional design.

Several toughening mechanisms were observed in the tree joint that were not present in the composite T-joint designs. CT scans illustrated tree joints have a unique internal structure with branch wood embedded into the centre of the trunk in a three-dimensional cone shape or ‘V notch’. This approach avoids an un-reinforced zone in the tree joint. The tree joint fails by pullout of the cone-shaped internal branch structure, initiated at the ‘joint seam,’ where the branch and trunk fibers interface.

Crack growth in the tree joint along the joint seam is highly controlled, explaining the high toughness and residual strength after peak load, observed in the stress curve. At the macro-level the cone-shaped fracture surfaces have interlocking corrugations that mechanically resist the sliding pullout of the branch. CT scans also revealed that there is a variation in density, or fiber volume fraction, across the tree joint, with highest density at the points of highest bending stress. Implementing a variable fiber

volume fraction may result in improved composite joint strength.

At the micro-level, scanning electron microscopy (SEM) and micro CT scanning showed wood cells at the tree joint exhibit significant fiber pullout and fiber bridging. Fiber pullout is a highly effective energy absorbing mechanism and fiber bridging reduces the stress at the crack tip that in turn promotes stable crack growth.

In comparison both the conventional and biomimetic aerospace T-joints had a resin rich zone or 'plug' as a consequence of the radius bend. This resin rich zone was the site of uncontrolled crack growth and brittle failure. Reducing or eliminating this resin rich zone, for example by mimicking the V notch as seen in the tree, may increase the toughness of the aerospace composite joints.

Contact Author Email Address

lauren.burns@student.rmit.edu.au

Acknowledgements

The author thanks Dr Stefanie Feih and Prof. Adrian Mouritz (RMIT University) for their assistance as PhD supervisors and Mr David Pook (Boeing Research & Technology Australia) for his assistance as industry advisor. The author also thanks Mr Ian Overend, Mr Peter Tkatchyk and Mr Bob Ryan (RMIT University) for technical support. Thanks to David Smith from Hancock Victoria Plantations for supplying the *Pinus radiata* wood specimens. Thanks to Central Melbourne Medical Imaging for the CT scans. The author acknowledges the technical, scientific and financial assistance from the AMMRF. The author acknowledges the financial support provided by the RMIT University Australian Postgraduate Award and Boeing Research and Technology.

Copyright Statement

References

1] Baldan A. Review: Adhesively bonded joints in metallic alloys, polymers and composite materials: Mechanical and environmental durability performance. *Journal of Materials Science*, 2004. 39: pp 4729 - 4797.

[2] Rispler A, Tong L, Steven P and Wisnom M. Shape optimisation of adhesive fillets. *Journal of Adhesion and Adhesives*, Vol. 20, No. 3, pp 221 - 231, 2000.

[3] Ball P. Shark skin and other solutions. *Nature*, Vol. 400, pp 507, 1999.

[4] Stanzl-Tschegg S. Microstructure and fracture mechanical response of wood. *International Journal of Fracture*, Vol. 139, pp 495 - 508, 2006.

[5] Jeronimidis G. The fracture behaviour of wood and the relations between toughness and morphology. *Proceedings of the Royal Society London*, Vol 208, pp 447 – 460, 1980.

[6] Shigo A., How tree branches are attached to trunks. *Canadian Journal of Botany*, Vol. 63, pp 1391 - 1401, 1985.

[7] Mueller U, Gindl W and Jeronimidis G. Biomechanics of a branch-stem junction in softwood. *Trees*, Vol. 20, pp 643 - 648, 2006.

[8] Jungnikl K, Goebbels J, Burgert I and Fratz P. The role of material properties for the mechanical adaptation at branch junctions. *Trees*, Vol. 23, pp 605 - 610, 2009.

[9] King M, Sutherland I and Le-Ngoc L. Fracture toughness of wet and dry Pinus radiata. *Holz als Roh- und Werkstoff*, Vol. 57, pp 235 - 240, 1999.

[10] Szekrenyes A and Jozsef U. Advanced beam model for fiber-bridging in unidirectional composite double-cantilever beam specimens. *Engineering Fracture Mechanics*, Vol. 72, pp 2686 - 2702, 2005.

[11] Bolza E and Kloot N. *The mechanical properties of 174 Australian timbers*. Melbourne, CSIRO, 1963.